Pergamon

Talanta, Vol. 41, No. 2, pp. 261–267, 1994

0039-9140/94 $6.00 + 0.00

ELECTRODEPOSITION AND STRIPPING PROCESS BY LONG OPTICAL PATHLENGTH POTENTIAL-STEP TRANSMISSION CHRONOABSORPTOMETRY

QINGJI XIE, XU CHENG, WANZHI WEI, LIHUA NIE and SHOUZHUO YAO*
Department of Chemistry and Chemical Engineering, Hunan University, Changsha 410082, P.R. China

(*Received* 21 *January* 1993. *Revised* 7 *July* 1993. *Accepted* 12 *July* 1993)

Summary—Based on the transmittance-averaged rather than absorbance-averaged model of long optical pathlength transmission spectroelectrochemistry, a reasonable theoretical model for potential-step electrodeposition and stripping process has been developed. It can accurately predict the stripping-chronoabsorptometric waveform with a peak absorbance with respect to the time rather than that with no peak but only a theoretical maximum absorbance at the initial stage of the stripping process. Cu(II) in $NH_3 \cdot H_2O$–NH_4Cl supporting electrolyte is utilized to verify the theory. With this anodic stripping spectroelectrochemical method, a detection limit of *ca* 0.01m*M* without stirring or *ca* 0.002m*M* under stirring during deposition can be achieved. An application in the analysis of copper in practical samples is presented.

Spectroelectrochemistry (SEC), which is the combination of spectroscopy and electrochemistry, has become a powerful method for the investigation of electrochemical processes.[1-3] Long optical pathlength transmission spectroelectrochemistry is a sensitive SEC technique compared with that using optically-transparent electrodes (OTEs).[4-8] In earlier work, an absorbance-averaged model was used, *i.e.*

$$A = \epsilon l w^{-1} \int_0^w C(x,t)\,dx \qquad (1)$$

where ϵ is the molar absorptivity (here suppose only one species absorbs), l is the optical pathlength, w is the width of the solution layer through which the incident light beam is passed, $C(x,t)$ is the concentration of the investigated species at a distance x from the working electrode surface at time t.

However, for a long optical pathlength mode in which the incident light beam passes parallel to rather than perpendicular to the working electrode surface, averaging transmittance rather than absorbance (though an absorbance-averaged spectroelectrochemical model is correctly used in the OTE case[1,2]) is assumed more reasonable and supported by experiments.[9,10] The equation connecting the absorbance with the concentration distribution is given by

$$A = \log w - \log \int_0^w 10^{-\epsilon l C(x,t)}\,dx,$$
$$\approx \log m - \log \sum_{i=1}^{m} 10^{-\epsilon l C_i} \qquad (2)$$

where m is the total number of volume elements into which the illuminated solution layer can be divided, C_i is the concentration in the ith volume element and i varies from 1 to m.

It is easy to find that equation (2) can be approximately changed into equation (1) only if the absorbance, *i.e.* $A = \epsilon l C(x,t)$, is small enough that the approximation equation $10^{-A} = 1 - A\ln(10)$ can be adopted (with a relative error smaller than about 3% for an absorbance smaller than 0.1). Thus (1) is only valid for smaller absorbance (*i.e.* $\epsilon l C(x,t)$ is smaller than about 0.1).

It seems that electrodeposition and anodic stripping analysis by long optical pathlength spectroelectrochemistry were first reported in Ref. 11. It was pointed out that the anodic stripping analysis by spectroelectrochemistry, in principle, could rival its voltammetric analogue, as it is not limited by the problem of distinguishing between Faradaic and non-Faradaic processes. Recently, theory for the electrodeposition and anodic stripping process has been reported where (1) was used to connect the absorbance with the concentration distribution.[12] Based on their assumptions, they have given the time-dependent absorbance for anodic

*To whom correspondence should be addressed.

stripping process under the semi-infinite diffusion condition and the initial condition of $C_o(x,0) = 0$ (*i.e.* the concentration of the metal ion is equal to zero everywhere at moment zero) as follows

$$A = A_o^{max} \operatorname{erf}[w/(4D_o t)^{\frac{1}{2}}] \quad (3)$$

where A_o^{max} is the maximum absorbance in the stripping chronoabsorptometric curve as well as the absorbance at the time nearly equal to zero, D_o is the diffusion coefficient of the oxidizing species.

However, equation (3) gives a maximum absorbance at the time nearly equal to zero while the error function gives a value of 1. Thus, it does not explain the experimental stripping-chronoabsorptometric waveform with a peak absorbance at a certain moment rather than the time near zero, as found in their paper. To our knowledge, it is due to the improper utilization of (1) to the stripping case, because $\epsilon l C_o(x,t)$ adjacent to the working electrode surface may be far larger than 0.1 at the initial stage of the stripping process. Thus, it is certainly of interest to improve their theoretical treatment.

In this paper, theoretical models for potential-step electrodeposition and anodic stripping process are established based on (2) and experimentally supported using Cu(II) in 0.2*M* $NH_3 . H_2O$–0.2*M* NH_4Cl supporting electrolyte. This method has also found application in the analysis of copper in practical samples.

THEORY

At first, assumptions are as follows:

(i) thickness of the deposited film can be approximately neglected;
(ii) as soon as the metal ion departs from the electrode surface during the stripping process, it reacts with the color-development reagent to form a light-absorbing species.

Then, electrodeposition and dissolution processes are discussed as follows.

Deposition process

For a potential step from no-electrodeposition potential to diffusion-controlled electrodeposition potential, the concentration of the soluble species is given as follows[13]

$$C_o(x,t) = C_o^* \operatorname{erf}[x/(4D_o t)^{\frac{1}{2}}] \quad (4)$$

and the Faradaic charge is

$$Q_d = 2nFSC_o^* (D_o t_d/\pi)^{\frac{1}{2}} \quad (5)$$

where S is the area of the working electrode surface, t_d is the deposition time, C_o^* is the bulk concentration of the oxidizing species, other symbols have their usual meanings.

Combination of equations (4) and (2) gives the theoretical time-dependent absorbance behavior during deposition process, *i.e.*

$$A = \log w - \log \int_0^w 10^{-\epsilon l C_o^* \operatorname{erf}[x/(4D_o t)^{\frac{1}{2}}]} \, dx. \quad (6)$$

Thus, knowing w and $\epsilon l C_o^*$, the diffusion coefficient, *i.e.* D_o, can be estimated from the chronoabsorptometric curves as in Ref. 10.

Potential-step stripping process

It is important to obtain the concentration distribution during the stripping process.

From an initial concentration distribution of $C_o(x,0) = 0$, because equation (3) was derived from (1) in Ref. 12, thus the concentration distribution during the stripping process may be assumed

$$C_o(x,t) = Q_d(nFS)^{-1}(\pi D_o t)^{-\frac{1}{2}} \exp[-x^2/(4D_o t)]$$
$$= 0.6366 C_o^* t_d^{\frac{1}{2}} t^{-\frac{1}{2}} \exp[-x^2/(4D_o t)] \quad (7)$$

Substituting equation (7) into (1) yields equation (3). However, substituting into equation (2) gives theoretical spectroelectrochemical behavior which is rather different from that obtained from equation (3) but in agreement with the experimental results with a peak absorbance at a certain time. Note, in fact, A_o^{max} in (3) can be easily obtained from equations (1), (5) and Faraday's law, *i.e.*

$$A_o^{max} = \epsilon l w^{-1} \int_0^w C_o(x,\tau) \, dx$$
$$= \epsilon l (wS)^{-1} Q_d/(nF)$$
$$= 1.1284 w^{-1} (D_o t_d)^{\frac{1}{2}} \epsilon l C_o^*$$
$$= K \epsilon l C_o^* \quad (8)$$

where $\tau \leqslant \tau_w$, τ_w is the time with a width of the diffusion layer equal to w, $K = 1.1284 w^{-1} (D_o t_d)^{\frac{1}{2}}$. In addition, K may be defined as a proportionality constant which may reflect the sensitivity variation of the spectroelectrochemical method compared to the conventional spectrophotometry, since the experimental peak absorbance, A_o^P, is approximately A_o^{max} under certain conditions, as discussed later.

To our knowledge, compared with the initial concentration of $C_o(x,0) = 0$, that of

$C_o(x,0) = C_o^* \mathrm{erf}[x/(4D_o t_d)^{\frac{1}{2}}]$ from equation (4), is easier to obtain experimentally by applying a tripping potential-step perturbation after a certain deposition time (*i.e.* t_d). It is more difficult to obtain the analytical solution of the concentration distribution during the stripping process for such an initial concentration distribution. However, with the help of a digital simulation of box methods reported by S. W. Feldberg,[14] this problem can also be solved.

At first, the normalized diffusion coefficient is given as

$$\bar{D}_o = D_o \Delta t/(\Delta x)^2 = 0.45 \qquad (9)$$

where Δx is defined by $\Delta x = w/m$.

If the stripping rate is fast enough that all the deposited substance can be completely stripped off into the first volume at moment Δt, then the concentrations at the first volume element and jth ($j \geqslant 2$) volume element at time Δt, *i.e.* $C_o(1,1)$ and $C_o(j,1)$, are given by

$$C_o(1,1) = C_o(1,0) + Q_d/(nFS\Delta x) + \bar{D}_o[C_o(2,0) - C_o(1,0)], \qquad (10)$$

$$C_o(j,1) = C_o(j,0) + \bar{D}_o[C_o(j+1,0) + C_o(j-1,0) - 2C_o(j,0)], \qquad (11)$$

where $C_o(j,0)$, $C_o(j+1,0)$ and $C_o(j-1,0)$ are the concentration distribution in jth, $(j+1)$th and $(j-1)$th volume element at time zero, respectively, *i.e.* the initial concentration distribution.

The concentrations at the first volume, jth volume ($j \geqslant 2$) at time $(k+1)\Delta t$ ($k \geqslant 1$) are given as follows

$$C_o(1,k+1) = C_o(1,k) + \bar{D}_o[C_o(2,k) - C_o(1,k)], \qquad (12)$$

$$C_o(j,k+1) = C_o(j,k) + \bar{D}_o[C_o(j-1,k) + C_o(j+1,k) - 2C_o(j,k)], \qquad (13)$$

where all the symbols have their usual meanings.

Thus the concentration distribution for this initial concentration and therefore the theoretical stripping-chronoabsorptometric results can be obtained according to equation (2).

EXPERIMENTAL

Instruments and reagents

The instruments were described previously.[10] The spectroelectrochemical cell is similar to those in Refs 11, 12. The working electrode was a glassy carbon plate. An Ag/AgCl saturated KCl reference electrode was immersed into the solution and put in intimate contact with the working electrode surface for the sake of small iR drop between them. A platinum foil, which served as the auxiliary electrode, was set to be parallel to the working electrode surface at a distance of *ca* 3 cm. The width of the transmitted light beam, which was confined between a blade with a sharp edge and the working electrode surface, were measured by an optical microscope with a determination precision of 2 μm. All potentials are reported with respect to the Ag/AgCl/KCl(sat.) reference electrode.

All reagents used were at least of analytical grade. The solutions of Cu(II) were prepared using $0.2M$ $NH_3 . H_2O$–$0.2M$ NH_4Cl as the supporting electrolyte. Doubly distilled water was used for all preparations. The experiments were done at room temperature.

An AST 386 computer was used to carry on all the programs which were written in Fortran. The programs are available from the authors.

Procedures

At first, the electrodes were washed using ethanol, acetone and doubly distilled water, then scanned repeatedly in the range -1.0 to 1.0 V until only slight and reproducible residual current could be found.

In our experiments, the sample solution was degassed with purified nitrogen at first, then the working electrode potential was set at -0.8 V to allow copper to electrodeposit on the working electrode surface at the diffusion-controlled rate in $NH_3 . H_2O$–NH_4Cl supporting electrolyte. For deposition under stirring, nitrogen stream was used to stir the solution through a tube (in a diameter of *ca* 3 mm for outlet) with a distance of *ca* 1 cm from the working electrode surface, and here the auxiliary electrode was isolated by a piece of porous glass. After a certain time, the electrodeposited copper was stripped off into the solution by adding a potential-step perturbation immediately. All the chronoabsorptometric curves were recorded at the wavelength of observation (here 600 nm) *in situ*. The spectroelectrochemical determination of the formal potential and the number of the electrons transferred was similar to that in Ref. 5. However, for a long optical pathlength thin-layer spectroelectrochemical cell used here, two plates of glassy carbon were used as the dual working electrode for the sake of faster

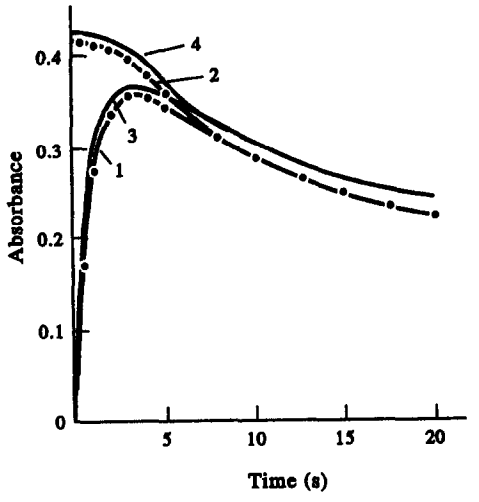

Fig. 1. Theoretical stripping-chronoabsorptometric curves. $\epsilon = 10{,}000$; $l = 1$ cm; $C_o^* = 0.00001M$; $w = 0.015$ cm; $D_o = 0.00001$ cm^2/sec; $t_d = 300$ sec. Curves: 1: $C_o(x,0) = 0$; from equation (2); 2: $C_o(x,0) = 0$; from equation (1); 3: $C_o(x,0) = C_o^* \mathrm{erf}[x/(4D_o t_d)^{\frac{1}{2}}]$; from equation (2); 4: $C_o(x,0) = C_o^* \mathrm{erf}[x/(4D_o t_d)^{\frac{1}{2}}]$, from equation (1). Lines: calculated from simulated results; dots: calculated from the analytical solution (*i.e.* equation (7)).

electrolysis owing to a larger (surface area)/(solution volume) ratio.

RESULTS AND DISCUSSIONS

Discussion of theoretical results

Theoretical spectroelectrochemical results are shown in Figs 1–4.

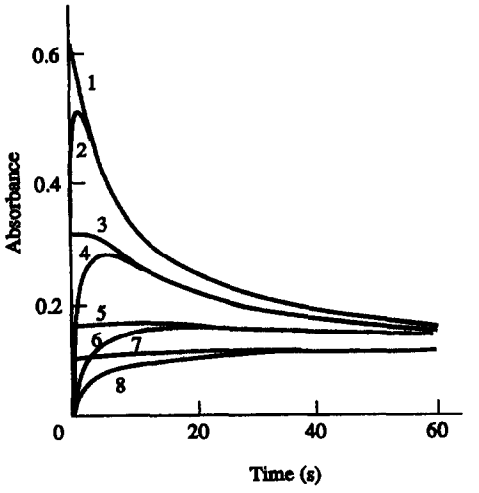

Fig. 2. Theoretical stripping-chronoabsorptometric curves for different values of w. $C_o(x,0) = 0$; $\epsilon = 10{,}000$; $l = 1$ cm; $C_o^* = 0.00001M$; $D_o = 0.00001$ cm^2/sec; $t_d = 300$ sec. w for each curve (cm): 1 and 2: 0.010; 3 and 4: 0.020; 5 and 6: 0.040; 7 and 8: 0.060. Curves 1,3,5,7: from equation (1); curves 2,4,6,8: from equation (2).

As can be seen from Figs 1 and 2, the theoretical stripping chronoabsorptometric curve from equation (2) differs severely from that of equation (1) at the initial stage of the stripping process but agrees well after some time. The stripping-chronoabsorptometric curve from (2) has a peak absorbance (*i.e.*, A_o^P) at certain time (*i.e.*, t_p) but the stripping-chronoabsorptometric curve from (1) has no peak absorbance but a maximum absorbance (*i.e.*, A_o^{max}) when the stripping process begins. Generally A_o^{max} is larger than A_o^P, moreover, a greater value of w can give a better agreement between A_o^{max} and A_o^P. Thus for greater values of w, A_o^P is approximately A_o^{max}, which can be calculated out in a simple way, *i.e.* from equation (8). However, greater values of w gives lower response of A_o^P and A_o^{max}, and, the time scale for the absorbance to reach A_o^P is also extended, *i.e.* t_p becomes larger. Thus the advantage to using a greater value of w in quantitative analysis is limited. Furthermore, the smaller the value of w is, the greater the peak absorbance (A_o^P) or the maximum absorbance (A_o^{max}) are, and, thus the more improved sensitivity is as in Fig. 2. Generally, the enhancement of the sensitivity due to electrodeposition can be several times or more. Thus, if an absorber with a molar absorptivity of 80,000 au/M/cm can be used, the detection limit can be calculated to be *ca* $1 \times 10^{-8}M$ with the value of w of 150 μm (provided the minimum measurable absorbance is three times that of absorbance uncertainty, *i.e.* 0.003). In addition, the differences of the stripping-chronoabsorptometric curves due to different initial concentration distribution are also shown in Fig. 1. It should be noted that the concentration distributions obtained either from equation (7) or from digital simulation under the condition of $C_o(x,0) = 0$ almost gives identical chronoabsorptometric curves. This conclusion may directly support our theoretical treatments where only digital simulation can be available.

Figure 3 is the plot of the peak absorbance and the maximum absorbance against the square root of the deposition time. Generally speaking, the longer the deposition time, the greater the peak absorbance and the maximum absorbance. In addition, a longer deposition time gives a greater difference between A_o^P and A_o^{max}. For an initial concentration distribution of $C_o(x,0) = 0$, there is a theoretically strict linear relationship between the maximum absorbance and the square root of the deposition

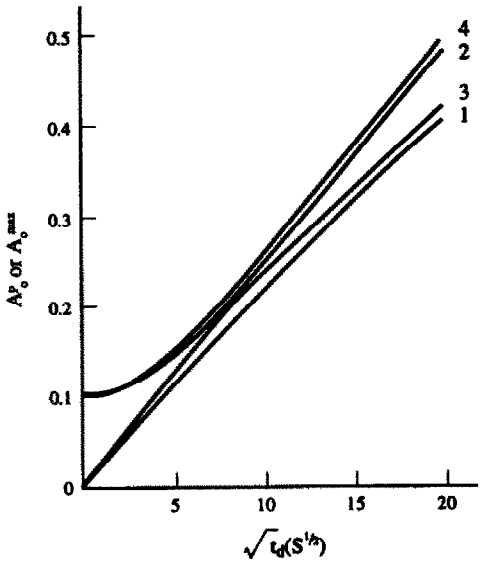

Fig. 3. Theoretical results of A_o^{max} and A_o^P for the square root of different values of deposition time. $\epsilon = 10000$; $l = 1$ cm; $C_o^* = 0.00001M$; $D_o = 0.00001$ cm²/sec. $w = 0.015$ cm. Curves: 1 and 3: from equation (2); 2 and 4: from equation (1); 1 and 2: $C_o(x,0) = 0$; 3 and 4: $C_o(x,0) = C_o^* \mathrm{erf}[x/(4D_o t_d)^{\frac{1}{2}}]$.

time according to (1), as predicted by (8). However, a strict linear relationship is not valid between them in the other three cases as shown by curve 1, curve 3 and curve 4 in Fig. 3.

Figure 4 is the plot of peak absorbance and the maximum absorbance against the bulk concentration of the deposited species during deposition. The conclusions are similar to that for Fig. 3. The greater the concentration, the greater the peak absorbance and the maximum

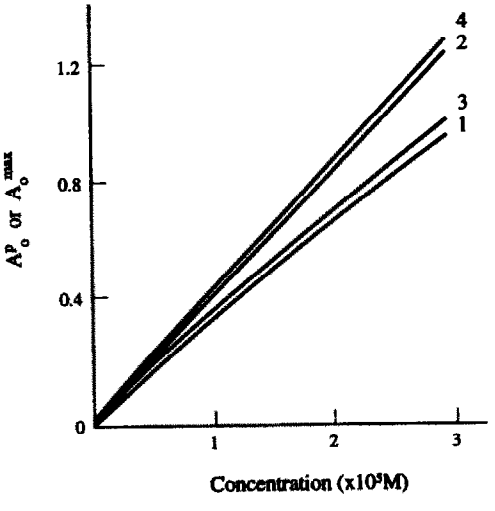

Fig. 4. Theoretical results of A_o^{max} and A_o^P for different values of bulk concentration C_o^*. $t_d = 300$ sec. Other conditions are the same as Fig. 3.

absorbance. Furthermore, a great value of C_o^* gives a more significant difference between A_o^P and A_o^{max}. Only for a small value of $\epsilon l C_o^*$ can A_o^P be almost equal to A_o^{max}, then (1) can be used instead of (2) for the stripping case, as pointed out previously. In addition, there is a theoretically strict linear relationship between the maximum absorbance and the bulk concentration in curves 2 and 4 according to (1). The other two curves, which are figured out from the correct transmittance-averaged model, *i.e.* equation (2), are not strict lines, and the greater the concentration, the more significant the curvature of the peak absorbance curve to the concentration axis. But, it is assumed that an approximate linear relationship still exists for each curve in a comparatively narrow range of the concentration, especially for that with peak absorbances smaller than *ca* 0.05. Thus, this spectroelectrochemical method can still find application in quantitative analysis with a linear regression model instead of a complicated nonlinear regression one over a narrow concentration range, which can be seen in curve 3.

Experimental support of model

In this work, Cu(II) in 0.2*M* $NH_3 . H_2O$–0.2*M* NH_4Cl supporting electrolyte was used to verify the theory.

At first, the formal potential and the number of the electrons of the electro-couple $Cu(NH_3)_4^{2+}/Cu(NH_3)_2^+$ were determined using a long optical pathlength thin layer spectroelectrochemical cell. The results of three determinations are $E^{o'} = -113$, -115, -112 mV; $n = 0.97$, 1.01, 0.98. Furthermore, it has been found that $\epsilon_{Cu(NH_3)_4^{2+}} = 52$ au/*M*/cm by our experiments.

In order to find the optimum deposition potential, we have investigated the effect of tuning the deposition potential on the stripping-chronoabsorptometric curves. Results show that the deposition process occurred over the potential range from *ca* -0.45 to -0.6 V. If more negative than -0.6 V, there were almost no differences among the stripping-chronoabsorptometric curves. However, if the deposition potential was negative to *ca* -1.2 V, gas bubbles were produced on the working electrode surface. Thus, the deposition potential was selected to be -0.8 V, the stripping potential is selected to be 0.30 V in our experiments. Furthermore, the diffusion coefficient of $Cu(NH_3)_4^{2+}$ can be obtained from the chronoabsorptometric curve during electrodeposition

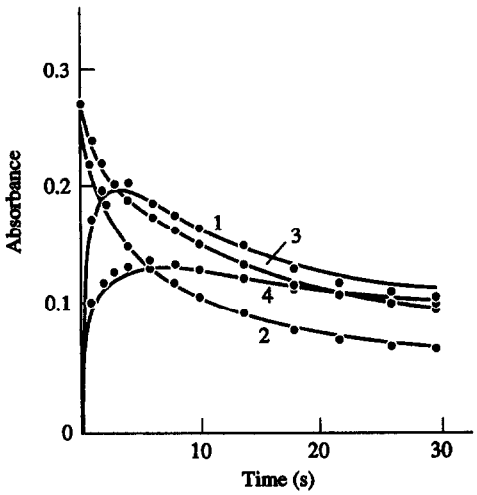

Fig. 5. Chronoabsorptometric curves during deposition (5 mM Cu(II), curves 2 and 3) and stripping process (1 mM Cu(II), curves 1 and 4) in 0.2M $NH_3 . H_2O - 0.2M$ NH_4Cl supporting electrolyte. Deposition potential (V): −0.8; stripping potential (V): 0.3. $l = 1.06$ cm; $t_d = 300$ sec; w (cm) for each curve: 1,2: 0.0156; 3,4: 0.0247. Lines: simulated results; dots: experimental results.

shown in Fig. 5 as in Ref. 10. Results in three trials are 9.47×10^{-6}, 9.56×10^{-6} and 9.69×10^{-6} cm^2/sec.

The stripping-chronoabsorptometric curves are shown in Fig. 5. It can be found that experimental stripping-chronoabsorptometric curves have a peak absorbance in the initial stage of the stripping process, which is accurately predicted by the theory developed in this work. Furthermore, good fits between the theoretical curves from equation (2) and the experiments were obtained, although some slight positive deviation were found in the peak value which may be ascribed to possible slight convection perturbation to the diffusion-controlled case during a long-time deposition, but the experimental responses deviate severely from the theoretical curves from (1) in the initial stage of the stripping process. This conclusion can also be found in Ref. 12, although most of their stripping experiments were done at the condition of initial concentration distribution equal to zero everywhere in the SEC cell.

Furthermore, our theory can also give some explanations about the experimental results in Ref. 12, which were the stripping-chronoabsorptometric curve of Cu(II) and CrO_4^{2-} in $NH_3 . H_2O$–NH_4Cl supporting electrolyte with an initial concentration distribution of zero and under the deposition condition without stirring. The theoretical model for electrodeposition and dissolution developed in this work can correctly explain the experimental peak absorbance at a certain time after dissolution. Furthermore, negative deviations at higher concentration (with peak absorbance greater than *ca* 0.05) from the linear relationship between the concentration and the peak absorbance can be found from the working curves in their work, and this phenomenon has been predicted by our theory shown in Fig. 4. However, it is unfortunate that their experimental A_0^P deviated severely from equation (8), for example, A_0^{max} in their Fig. 2, should be *ca* 0.02, but their experimental peak absorbance was *ca* 0.06. In our view, one of the causes may be the significant variations of the deposited layer due to the solution replacement with ammonia electrolyte after deposition since the amount of deposited substance on the electrode surface is very small.

Analytical application

It is certainly of interest to find application of the method to analyses of the practical samples. The experimental working curves without or under stirring were shown in Fig. 6. Obviously, because the copper quantity deposited on the electrode surface under stirring were greater than that without stirring for identical deposition durations, thus the sensitivity under stirring is apparently larger than that without stirring. The detectable limits are found to be about 0.002mM (under stirring) and 0.01mM (without stirring) from Fig. 6. The relative standard deviation for 1 mM without stirring

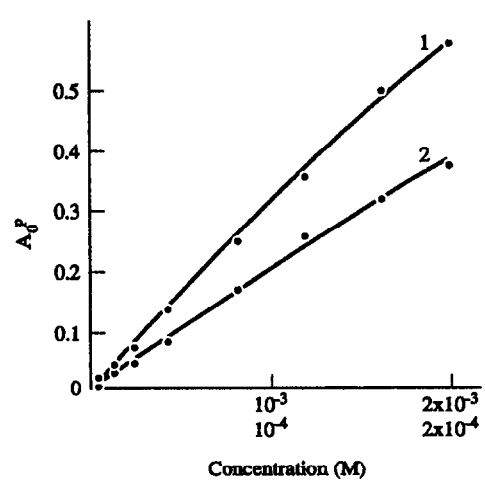

Fig. 6. Working curves. Deposition time: 300 sec; w (cm): 0.0142. $l = 1.51$ cm. Other conditions are the same as in Fig. 5. Curve 1: without stirring, upper concentration axis; curve 2: under nitrogen stirring with a flow rate of *ca* 30 ml/min, lower concentration axis.

Table 1. Determination results of copper

	True value	Found	Added	Recovery§
674 LD7		2.212%		97.5%
Aluminium	2.18%*	2.191%	1.00 m*M*	96.3%
alloy		2.131%		99.1%
675 LC4		1.693%		98.2%
Aluminium	1.66%*	1.654%	1.00 m*M*	97.3%
alloy†		1.659%		101.4%
Synthetic		0.214 m*M*		97.8%
water‡	0.232 m*M*	0.239 m*M*	0.200 m*M*	98.6%
		0.217 m*M*		97.4%

*Given by Shanghai Material Research Institute.
†Without stirring.
‡Under stirring.
§Based on incremental response after additional sample was added.

was 1.7% (12 times) and that for 0.1 m*M* under stirring was 2.4% (10 times). Thus we have tested copper in two aluminium alloys in which the contents of copper were given by Shanghai Material Research Institute and shown on the labels, and a synthetic water sample. The procedure for synthetic water was as above and that for aluminium alloy was as follows. Approximately 0.2 g sample was dissolved by certain amount of 0.1*M* HCl+ 10% H_2O_2, and after getting rid of extra acid by boiling it, a certain amount of *ca* 25% NaOH solution was added to separate copper from aluminium due to precipitated $Cu(OH)_2$ but soluble AlO_2^-. The precipitate was separated by a centrifuge or by filtering through a Shuangchuan-102 paper and then transferred into a beaker, 0.2*M* $NH_3 . H_2O$–NH_4Cl supporting electrolyte was added and the mixture was stirred vigorously to allow the complete conversion from $Cu(OH)_2$ to $Cu(NH_3)_4^{2+}$, and then the remaining precipitate was separated from the solution of $Cu(NH_3)_4^{2+}$ as above. Thus the solution was ready to be analyzed as above. Results are shown in Table 1. It can be seen that the determination results of copper by spectroelectrochemistry here are in agreement with the true values.

CONCLUSIONS

A reasonably long optical pathlength potential-step spectroelectrochemical model for electrodeposition and dissolution which can correctly explain the experimental stripping-chronoabsorptometric curve is presented. Cu(II) in $NH_3 . H_2O$–NH_4Cl supporting electrolyte was used to verify the theory. Copper in several practical samples has been determined by this method. Results show that the sensitivity of this method is significantly enhanced when compared to that without electrodeposition, and if suitable and sensitive color-development reagents are used, the detection limit can be down to *ca* $1 \times 10^{-8}M$. Further work in this field will be discussed in future papers.

Acknowledgements—Financial support from the National Science Foundation and Education Commission Fund of China is gratefully acknowledged.

REFERENCES

1. T. Kuwana and N. Winograd, *Electroanalytical Chemistry*, A. J. Bard (ed.) Vol. 7, p. 1. Marcel Dekker, New York, 1974.
2. W. R. Heineman, F. M. Hawkridge and H. N. Blount, *Electroanalytical Chemistry*, A. J. Bard (ed.), Vol. 13, p. 1. Marcel Dekker, New York, 1984.
3. R. J. Gale, *Spectroelectrochemistry: Theory and Practice*. Plenum Press, New York, 1988.
4. J. F. Tyson and T. S. West, *Talanta*, 1980, **27**, 335.
5. J. Zak, M. D. Porter and T. Kuwana, *Anal. Chem.*, 1983, **55**, 2219.
6. M. D. Porter and T. Kuwana, *Anal. Chem.*, 1984, **56**, 529.
7. P. Rossi and R. L. McCreery, *J. Electroanal. Chem.*, 1983, **151**, 47.
8. T. R. Nagy and J. L. Anderson, *Anal. Chem.*, 1991, **63**, 2668.
9. J. D. Brewster and J. L. Anderson, *Appl. Spectrosc.*, 1989, **43**, 710.
10. W. Wei, Q. Xie and S. Yao, *J. Electroanal. Chem.*, 1992, **328**, 9.
11. J. F. Tyson, *Talanta*, 1986, **33**, 51.
12. Y. Xie and S. Dong, *J. Electroanal. Chem.*, 1990, **294**, 21.
13. A. J. Bard and L. R. Faulker, *Electrochemical Methods: Fundamentals and Applications*. John Wiley, New York, 1980.
14. S. W. Feldberg, *Computers in Chemistry and Instrumentation*, Vol. 2, Chap. 7; *Electrochemistry*, J. S. Mattson, H. B. Mark and H. C. MacDonald (eds). Marcel Dekker, New York, 1972.